PAPER

Moisture and temperature influence on mechanical behavior of PPS/buckypapers carbon fiber laminates

To cite this article: J A Rojas *et al* 2017 *Mater. Res. Express* **4** 075302

View the article online for updates and enhancements.

Related content

- Processing, thermal and mechanical behaviour of PEI/MWCNT/carbon fiber nanostructured laminate
  L F P Santos, B Ribeiro, L R O Hein et al.

- Mechanical behavior of glass/epoxy composite laminate with varying amount of MWCNTs under different loadings
  K K Singh and Prashant Rawat

- Effect of surfactant on microstructure, surface hydrophilicity, mechanical and thermal properties of different multi-walled carbon nanotube/polystyrene composites
  Zhipeng Li, Yanxia Zhang, Shaolei Liang et al.

Recent citations

- Experimental investigation of transverse loading on composite panels coated with different gelcoat colors subjected to UV radiation and hygrothermal aging
  Akar Dogan *et al*

- Processing, thermal and mechanical behaviour of PEI/MWCNT/carbon fiber nanostructured laminate
  L F P Santos *et al*

IOP ebooks™

Bringing you innovative digital publishing with leading voices to create your essential collection of books in STEM research.

Start exploring the collection - download the first chapter of every title for free.

Materials Research Express

Moisture and temperature influence on mechanical behavior of PPS/buckypapers carbon fiber laminates

J A Rojas[1,2], L F P Santos[2], M L Costa[2], B Ribeiro[2] and E C Botelho[2]

[1] Technological Faculty—Mechanical Engineering, Universidad Distrital Francisco José de Caldas, Bogotá, Colombia
[2] Materials and Technology Department, School of Engineering, Universidade Estadual Paulista (UNESP), Guaratinguetá, Brazil

E-mail: jr21_6@hotmail.com

Abstract

In this work, multiwall carbon nanotubes (MWCNT) were dispersed in water with the assistance of water based surfactant and then sonicated in order to obtain a very well dispersed solution. The suspension was filtrate under vaccum conditions, generating a thin film called buckypapers (BP). Poly (phenylene sulphide) (PPS) reinforced carbon fiber (CF) and PPS reinforced CF/BP composites were manufactured through hot compression molding technique. Subsequently the samples were exposed to extreme humidity (90% of moisture) combined with high temperature (80 °C). The mechanical properties of the laminates were evaluated by dynamic mechanical analysis, compression shear test, interlaminar shear strength and impulse excitation of vibration. Volume fraction of pores were 10.93% for PPS/CF and 16.18% for PPS/BP/CF, indicating that the hot compression molding parameters employed in this investigation (1.4 MPa, 5 min and 330 °C) affected both the consolidation quality of the composites and the mechanical properties of the final laminates.

1. Introduction

Carbon fiber (CF) reinforced polymer composites have been widely employed in several sectors of industry, such as aerospace, automotive and aeronautical due their high specific strength and stiffness [1]. It is well known that delamination is one the primary damage issues associated in composites structures, causing severe reductions in its mechanical properties, potentially leading to catastrophic failure of the whole structure [2]. To further solve the issues pointed before hybrid composites have been introduced. Interleaving has been employed as crack arrester to break the continuity of crack propagation in fiber reinforced composites. Several types of interleaving materials have been developed, such as carbon nanotubes (CNT) or carbon nanofibers (CNF). Khan and Kim [3] reported an increase of about 31% of ILSS properties for multiscale composites containing CNF buckypaper (BP) interleaves. Therefore, the incorporation of nanomaterials as reinforcement in polymer composites is essential to understand the problems mentioned above identifying delamination initiation and avoid further propagation.

The introduction of nanofillers, such as CNT into polymer matrix is not a new concept [4]. Also, as studied for several researches [5–7], the addition of nanoscale particles in polymer matrix can generate materials with multi-functional features. One of the most employed nanoparticles used as reinforcement is the CNTs that posses excellent mechanical properties such as elastic modulus of (0.27–0.95) TPa, tensile resistance between 11 and 63 GPa [8–13] and low specific mass, which make them suitable to be used in aerospace structures, where the lightweight is one of the major goals looking for fuel saving [14–16].

The success of the incorporation of CNT in polymer composites depends basically on the adequate dispersion of the filler into polymer matrix. However, its low solubility in common solvents, strong agglomerating tendency to form bundles and aggregate together, due their high surface area and the strong van der Waals interaction, cause a poor dispersion and limits its practical applications [17–21].

In order to solve the problems concerning about the nanotubes dispersion, the use of CNT sheets (or BPs) can be considered as an alternative to the development of nanocomposites. The BP consists in thin surfaces with high porosity, generated by a macroscopic aggregate of CNTs [17]. Differently of traditional CNT-dispersed polymer composites, BP composites possess a dense network of CNT that acts like a skeleton inside the polymeric matrix [17, 22–24]. However, to obtain good mechanical properties, some factors during the composite processing must

be achieved such as an optimized BP impregnation, concentration and alignment of the nanoparticle, a strong interfacial CNT-polymer interaction and so on [25–27].

Despite the thermoset polymeric composites have greater demand in aerospace industry, the use of thermoplastic matrix arises like alternative. These materials have some advantages such as better, damage tolerance, chemical-environmental resistance, recycling possibilities, lower production costs and higher production rates in large volume markets such as construction, transportation and automotive. An important aspect to point, is that the average saturation gain (hygrothermal ageing) for thermoplastic composites is lower than for thermosetting laminates which is highly important in aerospace applications [28].

Inside of the high performance thermoplastics group used in aerospace industry can be found the poly (phenylene sulfide) (PPS). This polymer possesses good stability at elevated temperature combined with good mechanical properties, good chemical, oils and solvent resistance, high dimensional stability, inherent flame retardancy, relatively low material cost and good processability [29].

CNT reinforced PPS composites have been the subject of intensive research in recent years. Jiang *et al* [29] reported that the elastic modulus (*E*) and tensile strength were increased by 36 and 12%, respectively, in PPS filled with 8 wt% of multiwall carbon nanotube (MWCNT) and the flexural modulus and strength of PPS nanocomposites were increased by up to 20 and 14%, respectively. Yang *et al* [6] reported an increased in glass transition (Tg) and storage modulus values of PPS by adding MWCNTs, observed via DMA, and Díez-Pascual *et al* [30] reported remarkable improvement in the storage modulus of the PPS matrix of about 75% with the addition of 2.0 wt% of single walled carbon nanotubes (SWCNT) wrapped PEI (polyetherimide). This enhanced can be explained by the excellent SWCNT-PPS interfacial adhesion, which enables a more efficient stress transfer.

SWCNT-BP/PPS composites was manufactured by Diez-Pascual *et al* [18] that reported an increase in the storage modulus by 38%. Also, Tg increase by 26 °C and DMA results showed that the SWCNT-BP integrated composites exhibited higher stiffness and are thermomechanically more stable than neat PPS. The elastic modulus increased by 35% in good agreement with the results from DMA tests and the flexural moduli experienced about 24% enhancement. These significant increments indicate good interfacial adhesion between the two composite phases. For the reasons exposed above, the idea of fill PPS matrix with BPs can lead to a promising material in order to improve mechanical properties of this high performance thermoplastic matrix.

In this research, PPS matrix reinforced with BPs and CFs were manufactured. The temperature and moisture influence also have been evaluated on the mechanical and thermal properties of this nanocomposite material. Inside of this purpose, this material has been manufactured through hot compression molding processing. The thermal and mechanical properties have been evaluated by dynamic mechanical analysis (DMA), compression shear test (CST), interlaminar shear strength (ILSS) and impulsive excitation technique (IET).

2. Experimental

2.1. Materials
The composites used in this work were processed with plain weave CF woven with a weight of $129\,\mathrm{g\,m^{-2}}$ and density of $1.77\,\mathrm{g\,cm^{-3}}$ supplied by American Company Hexcel Composites. The PPS matrix was supplied by American Company Curbell Plastics in the form of films. Each film has about 0.125 mm of thickness and density of about $1.35\,\mathrm{g\,cm^{-3}}$, glass transition temperature of 85 °C and melting temperature of 285 °C. The CVD pristine MWCNTs were provided by Cheap Tubes Inc. ($d_{25\,°C} = 2.1\,\mathrm{g\,cm^{-3}}$, outer diameter: 8–15 nm, inside diameter: 3–5 nm, length: 10–50 μm). The polyamide membrane filters were provided by Membrane Solutions with diameter of around 45 mm. Also, a surfactant (Triton X-100) was used in this work in order to prevent the excessive agglomeration of the CNTs.

2.2. Preparation of BP reinforced composite laminate
90 mg of MWCNTs were first dispersed in 300 ml water with the aid of Triton X-100 surfactant and ultrasonicated for 30 min in order to form a well-dispersed and stable suspension. The CNT suspension was filtered under vaccum conditions through a membrane with a pore size of 0.45 μm. Subsequently, the polyamide filter with attached BP was submerged into a formic acid bath, in which the polyamide filter dissolved quickly. After being immersed in the bath for 20–30 min, the BP was transferred into another clean formic acid bath, in which it was immersed for 20–30 min. This process was repeated for 3–4 times to ensure effective and complete removal of the polyamide filter.

2.3. Preparation of PPS/BP/CF composite laminate
The PPS/BP/CF laminate was produced with 2.5 mm of thickness, attending the reinforcement/matrix volume content of 60/40 (v/v). Also, in order to obtain this result, 10 layers of PPS and 12 of reinforcement were required. Several obtained BP was placed in the central region of the laminate, between 2 layers of CF since that CNT loading in the final laminate was around 2.3wt.%. A schematic representation of the laminate disposition is presented in figure 1.
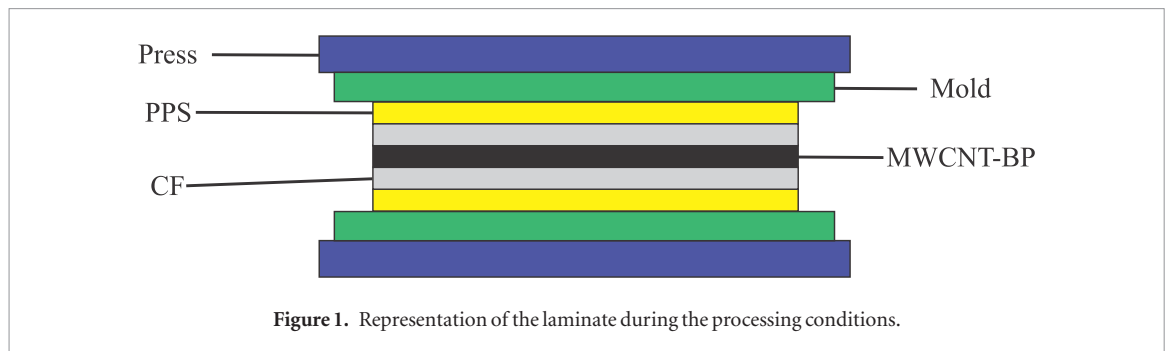
Figure 1. Representation of the laminate during the processing conditions.

The consolidation of the laminate was carried out in a hot press with controlled heating and cooling rate, (Carver brand, Monarch series, model CMV100H-15-X). The pressure, time and temperature used to produce the laminates were 1.4 MPa for 5 min and 330 °C, respectively. The heating rate to the dwell temperature was 5 °C min^{-1}, and the cooling to room temperature occurred slowly at a rate of 3 °C min^{-1}. For comparative purposes, a reference PPS/CF composite was prepared in same way. After the hot compression, the laminates were divided into four coupons as follows: PPS/CF (before the environmental conditioning), PPS/BP/CF (before the environmental conditioning), PPS/CF∗ (after conditioning), and PPS/BP/CF∗ (after conditioning).

2.4. Conditioning
Before the hygrothermal conditioning, the samples were maintained in oven at 100 °C for 24 h. This procedure was done in order to remove all the moisture of the sample to prevent the influence from the atmosphere humidity. The moisture absorption properties and equilibrium conditioning was based by ASTM D 5229/D 5229 M-04 standard. The samples were exposed at 80 °C and 90% relative humidity over a period of eight weeks. These parameters were programmed in Marconi MA 835/UR hygrothermal conditioning chamber. Every week, the specimens were removed from the chamber, weighed in a high precision balance to find the amount of water taken up and then put them back on the chamber. Water uptake was calculated as weight gained related to the weight of the dried specimen.

2.5. Dynamic mechanical analysis (DMA)
DMA analysis was performed to determine possible variations in the glass transition temperatures in the composite, storage modulus (E'), loss modulus (E'') and tan delta values. The DMA was carried out at a fixed frequency of 1 Hz, at the heating rate of 3 °C min^{-1} from 20 to 250 °C. Specimens for each situation were prepared with measures of 50 × 15 × 2.5 mm. These tests were performed in a SII Nanotechnology Exstar 6000 Thermal Analysis instrument.

2.6. Impulse excitation technique (IET)
The IET test can be used in order to obtain the modulus of elasticity of the composite by means of the method of natural frequencies of vibration that is based on ASTM E–1876 standard. The dimensions of the specimens used in this test were 50 × 15 × 2.5 mm. The tests were performed in Sonelastic equipment (Brazilian equipment). The parameters were calculated by using (1) and (2), where m is the mass, f_f is the natural frequency in the flexural dimension, b, L and t are the specimen width, length and thickness, respectively.

$$E = 0.9465 \left(\frac{m f_f^2}{b} \right) \left(\frac{L^3}{t^3} \right) T \tag{1}$$

$$T = 1 + 6.858 \left(\frac{t}{L} \right)^2. \tag{2}$$

2.7. Short beam (ILSS)
The ILSS test method determines the transverse shear load experienced by a composite material. The test is based on ASTM D 2344/D 2344 M-16 standard. Specimens with 16 × 7 × 2.5 mm of dimension were used in this test. The tests were performed in an universal Shimatzu mechanical tests machine, (Autograph AG-X series), with test speed of 1.0 mm min^{-1} and a load cell of 10 KN. The ILSS was calculated with (3), where P is the failure load, b and h are the specimen width and thickness, respectively.

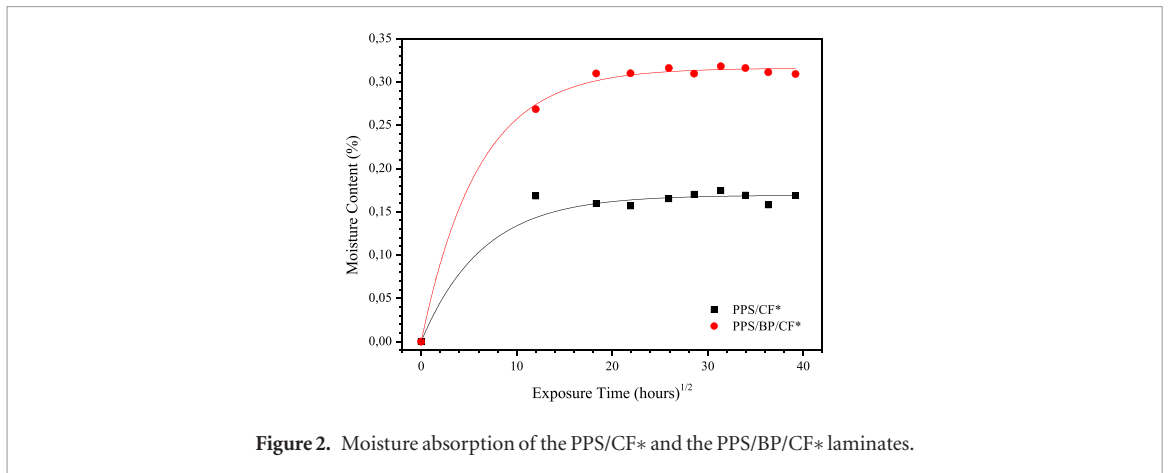$$\text{ILSS} = \frac{0.75 \, P}{bh}. \tag{3}$$

Figure 2. Moisture absorption of the PPS/CF∗ and the PPS/BP/CF∗ laminates.

2.8. Compression shear test (CST)

The CST is designed to generate direct shear load along the inter-laminate interface and force the specimen to break apart in pure shear. The shear stress distribution is almost uniform through the thickness with two peaks near the loading surface edges. By means of this test can be obtained Force–Displacement Apparent shear stress–displacement graphs [31]. Specimens for each situation were evaluated by CST, measuring ($10 \times 10 \times 2.5$) mm and the tests were carried out in an universal Shimatzu mechanical tests machine, (Autograph AG-X series), with test speed of 1.0 mm min^{-1} and a load cell of 5 KN.

2.9. Calculation of density and porosity of the composite laminate

The volume fraction of pore of the PPS/CF ($v_{p \, (PPS/CF)}$) and the PPS/BP/CF ($v_{p \, (PPS/BP/CF)}$) composites, can be estimated according to (4) and (5), respectively, as suggested by Ashrafi *et al* [32] and Han *et al* [33]:

$$v_{p(PPS/CF)} = 1 - v_{PPS} - v_{CF} = 1 - \frac{\rho_{PPS/CF} \cdot w_{PPS}}{\rho_{PPS}} - \frac{\rho_{PPS/CF} \cdot w_{CF}}{\rho_{CF}} \tag{4}$$

$$v_{p(PPS/BP/CF)} = 1 - v_{PPS} - v_{CF} - v_{BP} = 1 - \frac{\rho_{PPS/BP/CF} \cdot w_{PPS}}{\rho_{PPS}} - \frac{\rho_{PPS/BP/CF} \cdot w_{CF}}{\rho_{CF}} - \frac{\rho_{PPS/BP/CF} \cdot w_{BP}}{\rho_{BP}}. \tag{5}$$

Where v_{PPS}, v_{Cf} and v_{BP} are the volume fraction of PPS, CF and BP in the composite; ρ_{PPS} is the density of the PPS and equals to 1.35 g cm^{-3}; ρ_{CF} is the density of the CF and equals to 1.77 g cm^{-3}; $\rho_{PPS/CF}$ is the density of the PPS/CF composite, which is obtained by dividing the mass of a composite sample by its volume; w_{PPS} and w_{CF} are the weigh fraction of the PPS and CF in the composite. For the (5), $\rho_{PPS/BP/CF}$ is the density of PPS/CF/BP composite, which is obtained by dividing the mass of a composite sample by its volume; w_{BP} is the weight fraction of the BP in the composite and ρ_{BP} is the density of the as-prepared BP, which is estimated to be 0.46 g cm^{-3}, agree with the BP density reported in the literature [32, 34]. Scanning electron microscopy (SEM) was used to compare the impregnation grade between the PPS, BP and CF reinforcement and the composites defects, this was carried out in a FEI Inspect S50 microscopy.

3. Results and discussions

Figure 2 shows the curves obtained during the hygrothermal conditioning for the PPS/CF∗ and PPS/BP/CF∗ laminates. As it was expected, both cases show an initial linear region corresponding to a steady rate of moisture absorption up to a flat plateau. This means that, the specimens presented a weight gain during the exposure time since the water remains free over time and tends to penetrate in polymer matrix by the concentration gradient. Also, it initiates the relaxation process of the polymer chain and the hygrothermal filling of existing voids [35, 36]. In this work, it was observed that after eight weeks of exposure in moisture environment the composites presented the follow average values of saturation points: the PPS/CF∗ laminate presented 0.165% and the PPS/BP/CF∗ laminate reached 0.307% of moisture, respectively. As can be observed the PPS/BP/CF∗ had a higher percentage of moisture absorbed due to MWCNT-BP. This behavior can be explained since the MWCNT are randomly oriented through the BP, parallel to the surface of the sample, creating a network between them that gives rise to small pores that were subsequently filled with water [37, 38]. Also, as can be noted in figure 3 it seems PPS is not correctly impregnated to MWCNT-BP. According to previous works [39] the wettability of the BP to polymer matrix is the key factor when it is used as interleaf. Since the dark central zone corresponds to the BP and the external zones correspond to the CF (needles and points) and the PPS matrix, it can be concluded that BP was not correctly impregnated in PPS during the hot compression procedure. This situation can lead to a weak interfacial
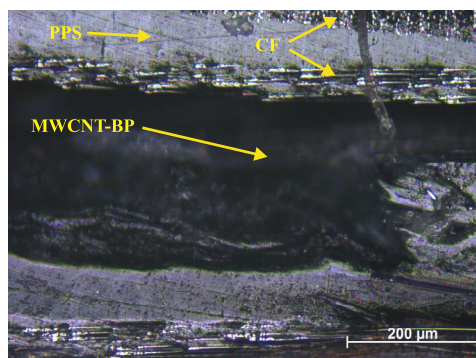
Figure 3. Photomicrography of the PPS/BP/CF.
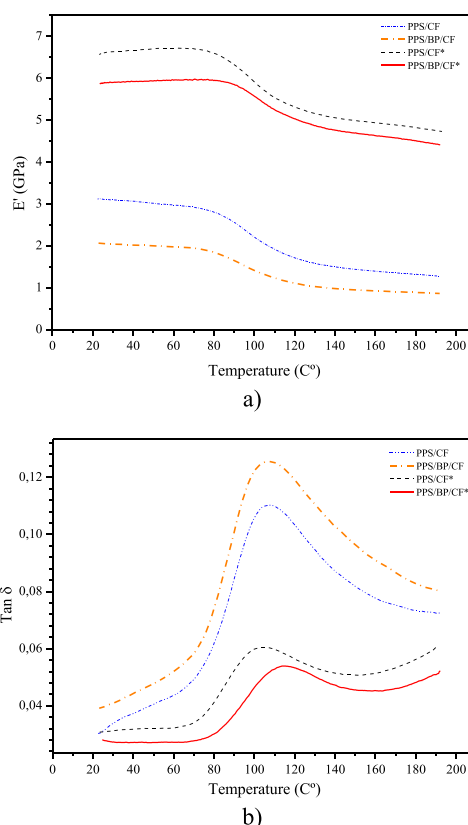

a)

b)

Figure 4. Representative DMA curves of the PPS/CF, PPS/BP/CF, PPS/CF∗ and PPS/BP/CF∗: (a) storage modulus; (b) tan delta.

CNT-polymer interaction, increasing the moisture absorption and consequently, prejudicing the mechanical properties of the laminate.

Figures 4(a) and (b) show the results corresponding to the viscoelastic properties measured by DMA of PPS/CF and PPS/BP/CF laminates before and after the hygrothermal conditioning. The values of the storage modulus (E') at 25 °C and Tg are collected in table 1. As can be noted in table 1 PPS/BP/CF laminate shown a decrease of about 51% in E' when its compared to PPS/CF system. As mentioned above, a lack of wettability between BP and PPS implies in a weak interfacial CNT-polymer interaction, compromising the storage modulus of BP composite. On the other hand, after the conditioning it turns out the increase in E' is associated with some kind of stiffening effect in the samples. As can be seen PPS/CF∗ laminate presented an increase of about 112% whereas PPS/BP/CF system shown a huge increment up to 186%. This behavior can be associated with degradation of the material or a creation of secondary crosslinking network, which means that the mixture of water and high temperature does not act properly as plasticize making the samples more rigid [40]. Furthermore, it can be noted that the Tg is only affected in PPS/BP/CF∗ system by the increase of ~7 °C, i.e. a 6% increment in the value of the glass transition temperature after the hygrothermal conditioning. These changes of Tg imply a lower mobility in the polymer chains of the material [40], compared to the other samples that are in the range of ~107 °C (also depicted in table 1) and as reported in previous works [41].

Table 1. Values of E obtained from IET measurements, E' and Tg obtained from DMA measurements and ILSS measurements.

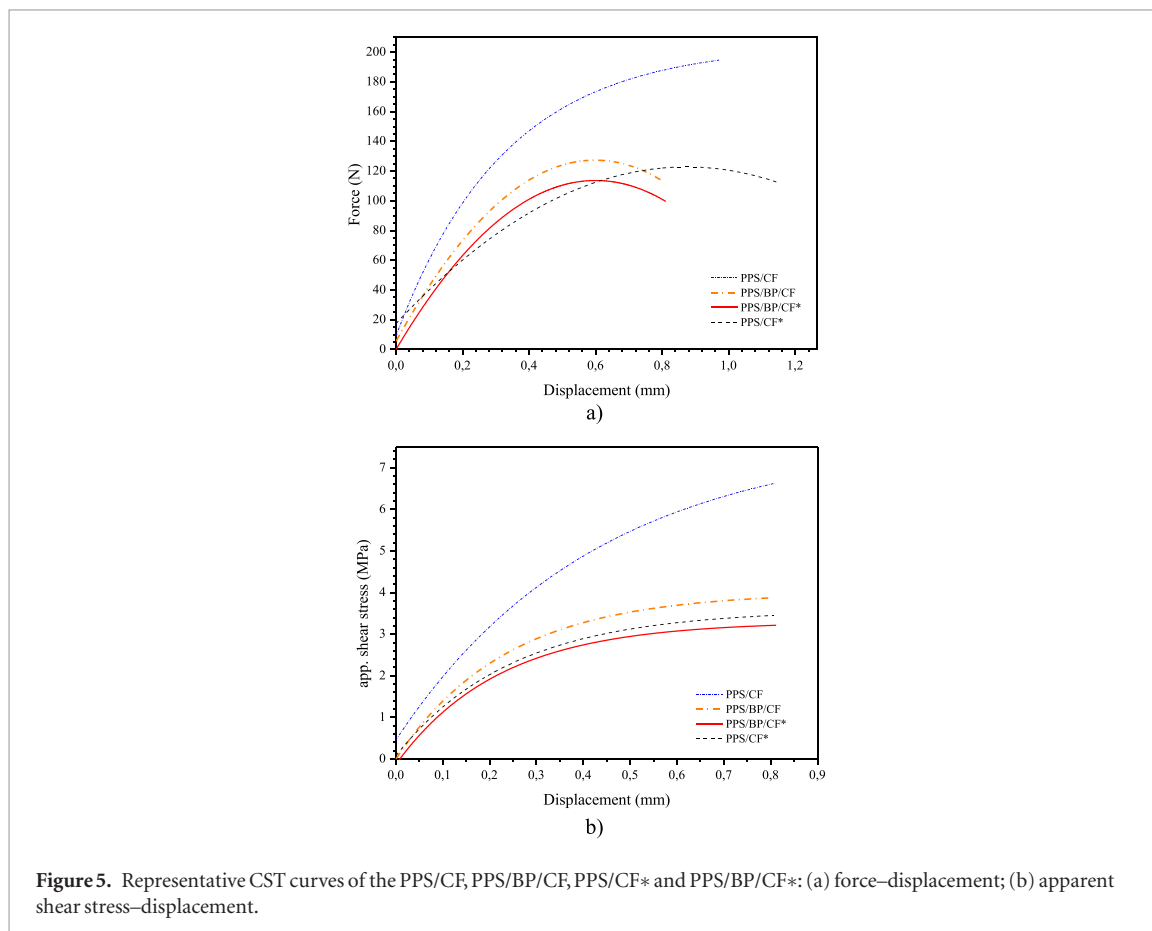| Sample	E (GPa)	E'25 °C (GPa)	Tg (°C)	ILSS (MPa)
PPS/CF	29.39	3.11	107	21.84 ± 3.71
PPS/CF*	57.36	6.61	105	16.00 ± 0.64
PPS/BP/CF	24.38	2.05	107	9.41 ± 1.55
PPS/BP/CF*	28.57	5.87	114	11.48 ± 0.74

Figure 5. Representative CST curves of the PPS/CF, PPS/BP/CF, PPS/CF* and PPS/BP/CF*: (a) force–displacement; (b) apparent shear stress–displacement.

Table 1 presents the results from the modulus of elasticity (E) obtained from the IET test. It can be seen that the PPS/CF* presented an increase in E of ~49% compared to the same composite before conditioning. The values obtained were lower than those reported in previous studies [41]. Analogously, the PPS/BP/CF* also showed an increase in E of ~15%, when compared to PPS/BP/CF before conditioning. The results are consistent with the values obtained by DMA.

The results corresponding to ILSS test are shown in table 1. It can be seen that the PPS/CF* presented a decrease in ILSS of ~27%. The decrease is related to form with which water molecules was absorbed by the material and how the water molecules were bound to the polymer chain and migrated to the interface [42]. On the other hand, the results for PPS/BP/CF* have a small increase in shear strength compared to the same sample before conditioning. However, considering the standard deviation, the results are practically the same, which means that the hygro-thermal conditioning does not affect the material. In figure 5 is depicted the curves recorded during the CST tests. The concentration of the stress is directed along the direction of the fiber, because the resistance is higher in this direction, in the case of PPS/CF. On the other hand, the incorporation of BP acts as a stress concentrator instead of reinforcement in the PPS/BP/CF material, resulting in less resistance to interlaminar shear.

In all the tests performed (DMA, IET, ILSS, CST) the PPS/BP/CF and the PPS/BP/CF* presented a reduction in their mechanical properties as a result of the defects caused by the poor impregnation of the BP, as was already said. Due the issues pointed above, the direct comparison between the laminates is difficult, making the obtained results atypical, particularly the ILSS data in table 1 and the curves of CST (figure 5). When reviewing the failure zones of some samples (figure 7), it can be seen that the darker areas can be associated to MWCNT-BP and the clearest areas correspond to the CF. Therefore, it can be seen that the delamination probably occurs in the area where the MWCNT-BP is located. As mentioned above, the interfacial adhesion between CNT and PPS matrix plays a key role in composite materials. Since the processing parameters such as pressure (1.4 MPa) and short pressing time
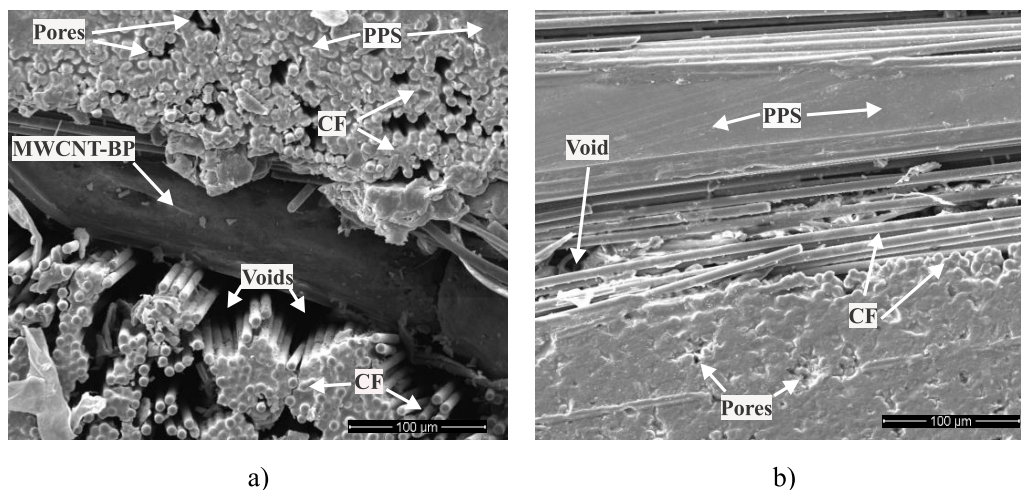
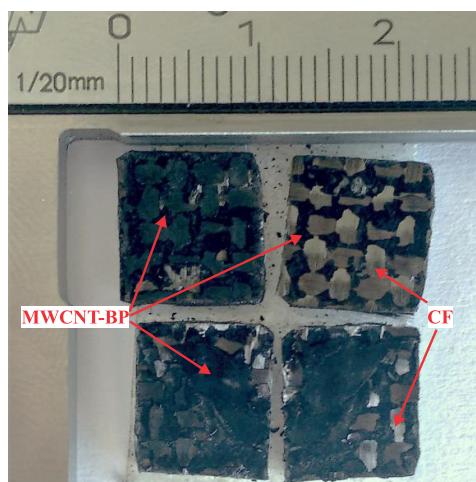**Figure 6.** SEM images of the (a) PPS/BP/CF and (b) PPS/CF.

Figure 7. Failure of the PPS/BP/CF.

Table 2. Density and volume fraction pore of the PPS/CF and PPS/BP/CF.

Sample	Density (g cm^{-3})	Volume fraction pore (%)
PPS/CF	1.38 ± 0.06	10.93
PPS/BP/CF	1.23 ± 0.07	16.18

(5 min) were not optimized, the BP was not incorporated successfully in PPS, as can be seen in figure 6(a), where there are a lot of voids and pores between the BP and the CF, leading to a reduction in mechanical parameters compared to the PPS/CF system figure 6(b). Density and volume fraction pore calculations shows that the PPS/BP/CF has more pore volume fraction and less density than PPS/CF, as can be seen in table 2. Therefore, it is easy to conclude that due to the lack of PPS impregnation in the MWCNT-BP, this zone has more pores, that acts as load concentrators, which did not allow an adequate interface between the matrix, the nanofiller and the CF. This led to the absence of the expected load distribution for this type of composites [17, 18, 43]. In addition, other key factors can explain the material behavior in this work. Pressures of 40 and 130 bars were reported by Díez-Pascual *et al* [43] that compared to this work, are much greater. Another important fact is that the pressing time could not have been so long enough to impregnate the BP, contributing to lower mechanical properties.

4. Conclusions

The mechanical and thermal properties of high-performance PPS/CF and PPS/CF based laminates incorporating randomly oriented MWCNT-BP were analyzed. According the obtained results the processing parameters used

in the study (pressure of 1.4 MPa and short pressing time 5 min) were not adequate for the consolidation of the laminate, leading to an insufficient mechanical behavior of the PPS/BP/CF composite.

The DMA studies revealed that the conditioned samples presented an increase in storage modulus. Similarly, IET test showed an increase in modulus of elasticity, also for the conditioned samples. This is possibly by some type of stiffening during the hygrothermal conditioning. On the other hand, the data obtained by the ILSS test indicate that the samples with MWCNT-BP are not affected by the hygrothermal conditioning. A Different case occurred with the PPS/CF laminate which had a decrease in the interlaminar shear resistance after conditioning. The mechanical properties of PPS/BP/CF were affected by the lack of impregnation between PPS and MWCNT-BP. This behavior can be associated by the processing parameters, as mentioned above. For this reason, MWCNT-BP probably acted as a load concentrators that allowed the delamination of the material and not as a reinforcement as would be expected. The results presented in this work open up new opportunities to optimize the impregnation and manufacturing processes of PPS matrix composite, reinforced with CF and MWCNT-BP. Further studies varying the pressure and pressing time of molding should be made to evaluate the best processing parameters for the PPS / MWCNT-BP composite.

Acknowledgments

References

[1] Costa G G Da, Botelho E C, Rezende M C and Costa M L 2008 Avaliação do ciclo térmico de conformação por compressão de peças em poli (sulfeto de fenileno) reforçado com fibras contínuas de carbono *Polímeros* **18** 81–6

[2] Liu L, Wu J and Zhou Y 2016 Enhanced delamination initiation stress and monitoring sensitivity of quasi-isotropic laminates under in-plane tension by interleaving with CNT buckypaper *Compos. A* **89** 10–7

[3] Khan S U and Kim J K 2012 Improved interlaminar shear properties of multiscale carbon fiber composites with bucky paper interleaves made from carbon nanofibers *Carbon* **50** 5265–77

[4] de Paiva L B, Morales A R and Guimarães T R 2006 Propriedades mecânicas de nanocompósitos de polipropileno e montmorilonita organofílica *Polímeros* **16** 136–40

[5] Chandrasekaran V C S, Advani S G and Santare M H 2010 Role of processing on interlaminar shear strength enhancement of epoxy/glass fiber/multi-walled carbon nanotube hybrid composites *Carbon* **48** 3692–9

[6] Yang J, Xu T, Lu A, Zhang Q, Tan H and Fu Q 2009 Preparation and properties of poly (p-phenylene sulfide)/multiwall carbon nanotube composites obtained by melt compounding *Compos. Sci. Technol.* **69** 147–53

[7] Cho M H and Bahadur S 2007 A study of the thermal, dynamic mechanical, and tribological properties of polyphenylene sulfide composites reinforced with carbon nanofibers *Tribol. Lett.* **5** 237–45

[8] Yakobson B I, Brabec C J and Bernholc J 1996 Nanomechanics of carbon tubes: Instabilities beyond linear response *Phys. Rev. Lett.* **76** 2511–4

[9] Robertson D H, Brenner D W and Mintmire J W 1992 Energetics of nanoscale graphitic tubules *Phys. Rev. B* **45** 12592

[10] Krishnan A, Dujardin E, Ebbesen T W, Yianilos P N and Treacy M M J 1998 Young's modulus of single-walled nanotubes *Phys. Rev. B* **58** 14013–9

[11] Treacy M M J, Ebbesen T W and Gibson J M 1996 Exceptionally high Young's modulus observed for individual carbon nanotubes *Nature* **381** 678

[12] Wong E W, Sheehan P E and Lieber C M 1997 Nanobeam mechanics: elasticity, strength, and toughness of nanorods and nanotubes *Science* **277** 1971–5

[13] Demczyk B G *et al* 2002 Direct mechanical measurement of the tensile strength and elastic modulus of multiwalled carbon nanotubes *Mater. Sci. Eng. A* **334** 173–8

[14] Anazawa K, Shimotani K, Manabe C, Watanabe H and Shimizu M 2002 High-purity carbon nanotubes synthesis method by an arc discharging in magnetic field *Appl. Phys. Lett.* **81** 739–41

[15] Díez-Pascual A M *et al* 2009 Development and characterization of PEEK/carbon nanotube composites *Carbon* **47** 3079–90

[16] Valter B, Ram M K and Nicolini C 2002 Synthesis of multiwalled carbon nanotubes and poly (o-anisidine) nanocomposite material: fabrication and characterization of its Langmuir − Schaefer films *Langmuir* **18** 1535–41

[17] Wang Z, Liang Z, Wang B, Zhang C and Kramer L 2004 Processing and property investigation of single-walled carbon nanotube (SWNT) buckypaper/epoxy resin matrix nanocomposites *Compos. A* **35** 1225–32

[18] Díez-Pascual A M, Guan J, Simard B and Gómez-Fatou M A 2012 Poly(phenylene sulphide) and poly(ether ether ketone) composites reinforced with single-walled carbon nanotube buckypaper: II—mechanical properties, electrical and thermal conductivity *Compos. A* **43** 1007–15

[19] Disfani M N and Jafari S 2013 Assessment of intertube interactions in different functionalized multiwalled carbon nanotubes incorporated in a phenoxy resin *Polym. Eng. Sci.* **53** 168–75

[20] Ma P-C, Siddiqui N A, Marom G and Kim J-K 2010 Dispersion and functionalization of carbon nanotubes for polymer-based nanocomposites: a review *Compos. A* **41** 1345–67

[21] Díez-Pascual A M *et al* 2010 High performance PEEK/carbon nanotube composites compatibilized with polysulfones-I. Structure and thermal properties *Carbon* **48** 3485–99

[22] Ashrafi B *et al* 2012 Processing and properties of PEEK/glass fiber laminates: effect of addition of single-walled carbon nanotubes *Compos. A* **43** 1267–79

[23] Zhang J and Jiang D 2012 Influence of geometries of multi-walled carbon nanotubes on the pore structures of Buckypaper *Compos. A* **43** 469–74

[24] Feng Q-P, Yang J-P, Fu S-Y and Mai Y-W 2010 Synthesis of carbon nanotube/epoxy composite films with a high nanotube loading by a mixed-curing-agent assisted layer-by-layer method and their electrical conductivity *Carbon* **48** 2057–62

[25] Liu L, Shen L and Zhou Y 2016 Improving the interlaminar fracture toughness of carbon/epoxy laminates by directly incorporating with porous carbon nanotube buckypaper *J. Reinf. Plast. Compos.* **35** 165–76

[26] Fu X, Zhang C, Liu T, Liang R and Wang B 2010 Carbon nanotube buckypaper to improve fire retardancy of high-temperature/high-performance polymer composites *Nanotechnology* **21** 235701

[27] Dalina W A D W, Tan S H and Mariatti M 2016 Properties of fiberglass/MWCNT buckypaper/epoxy laminated composites *Proc. Chem.* **19** 935–42

[28] Franco L A L, Graça M L A and Silva F S 2008 Fractography analysis and fatigue of thermoplastic composite laminates at different environmental conditions *Mater. Sci. Eng.* A **488** 505–13

[29] Jiang Z, Hornsby P, Mccool R and Murphy A 2011 Mechanical and thermal properties of polyphenylene sulfide/multiwalled carbon nanotube composites *Appl. Polym. Sci.* **123** 2676–83

[30] Díez-Pascual A M, Naffakh M, Marco C and Ellis G 2012 Mechanical and electrical properties of carbon nanotube/poly (phenylene sulphide) composites incorporating polyetherimide and inorganic fullerene-like nanoparticles *Compos.* A **43** 603–12

[31] Schneider K, Lauke B and Beckert W 2001 Compression shear test (CST)—a convenient apparatus for the estimation of apparent shear strength of composite materials *Appl. Compos. Mater.* **8** 43–62

[32] Ashrafi B, Guan J, Mirjalili V, Hubert P, Simard B and Johnston A 2010 Correlation between Young's modulus and impregnation quality of epoxy-impregnated SWCNT buckypaper *Compos.* A **41** 1184–91

[33] Han J-H, Zhang H, Chen M-J, Wang G-R and Zhang Z 2014 CNT buckypaper/thermoplastic polyurethane composites with enhanced stiffness, strength and toughness *Compos. Sci. Technol.* **103** 63–71

[34] Mechrez G, Suckeveriene R Y, Tchoudakov R, Kigly A, Segal E and Narkis M 2012 Structure and properties of multi-walled carbon nanotube porous sheets with enhanced elongation *J. Mater. Sci.* **47** 6131–40

[35] Costa A P, Botelho E C and Pardini L C 2010 Influence of environmental conditioning on the shear behavior of poly(phenylene sulfide)/glass fiber composites *J. Appl. Polym. Sci.* **118** 180–7

[36] de Faria M C M, Appezzato F C, Costa M L, de Oliveira P C and Botelho E C 2011 The effect of the ocean water immersion and UV ageing on the dynamic mechanical properties of the PPS/glass fiber composites *J. Reinf. Plast. Compos.* **30** 1729–37

[37] Hussein L, Urban G and Krüger M 2011 Fabrication and characterization of buckypaper-based nanostructured electrodes as a novel material for biofuel cell applications *Phys. Chem. Chem. Phys.* **13** 5831–9

[38] Trakakis G, Tasis D, Aggelopoulos C, Parthenios J, Galiotis C and Papagelis K 2013 Open structured in comparison with dense multi-walled carbon nanotube buckypapers and their composites *Compos. Sci. Technol.* **77** 52–9

[39] Song L, Zhang H, Zhang Z and Xie S 2007 Processing and performance improvements of SWNT paper reinforced PEEK nanocomposites *Compos.* A **38** 388–92

[40] Batista N L, de Faria M C M, Iha K, de Oliveira P C and Botelho E C 2015 Influence of water immersion and ultraviolet weathering on mechanical and viscoelastic properties of polyphenylene sulfide-carbon fiber composites *J. Thermoplast. Compos. Mater.* **28** 340–56

[41] de Souza S D B, Abrahão A N A, Costa M L, Marlet J, Hein L and Botelho E C 2016 Experimental investigation of processing welding parameters for PPS/carbon fiber laminates for aeronautical applications *Adv. Mater. Res.* **1135** 62–74

[42] Costa A P, Botelho E C and Pardini L C 2011 Efeito da degradação ambiental nas propriedades de cisalhamento de compósitos PPS/fibra de carbono *Polímeros* **21** 161–7

[43] Díez-Pascual A M, Guan J, Simard B and Gómez-Fatou M A 2012 Poly (phenylene sulphide) and poly (ether ether ketone) composites reinforced with single-walled carbon nanotube buckypaper: I—structure, thermal stability and crystallization behaviour *Compos.* A **43** 997–1006